

# Analog Signal Processing in Transmission Line Metamaterial Structures

*Shulabh GUPTA, Christophe CALOZ*

Poly-Grames Research Center, École Polytechnique de Montréal, Montréal, Québec, Canada

shulabh.gupta@polymtl.ca

**Abstract.** Several novel dispersion-engineered CRLH TL metamaterial analog signal processing systems, exploiting the broadband dispersive characteristics and design flexibility of CRLH TLs, are presented. These systems are either guided-wave or radiated-wave systems, and employ either the group velocity or the group velocity dispersion parameters. The systems presented are: a frequency tunable impulse delay line, a pulse-position modulator, a frequency discriminator and real-time Fourier transformer, pulse generators, an analog real-time spectrum analyzer, a frequency-resolved electrical gating, a spatio-temporal Talbot effect imager, and analog true-time delay. They represent a new class of impulse-regime metamaterial structures, while previously reported metamaterials were mostly restricted to the harmonic regime.

## Keywords

Analog signal processing, dispersion engineering, transmission line metamaterials, leaky-wave antennas, Talbot effect, real-time spectrum analyzers, pulse-position modulators, real-time Fourier transformation, true-time delay.

## 1. Introduction

Metamaterial structures [1], thanks to their inherent dispersive nature, have extended the possibilities of dispersion engineering, relatively common in optics [2], to microwave systems. Dispersion engineering consists in shaping the phase of electromagnetic waves to process signals in an analog fashion, leading to applications such as real-time Fourier transformers, pulse shapers, convolvers and correlators. This approach is particularly useful in applications where digital solutions are not available, as for instance in very high frequency and high speed ultra-wideband microwave systems. At microwaves, a very long history of “magnitude engineering” in the form of filter theory and techniques exists, but no systematic approach has been reported for dispersion engineering, except for all-pass filters restricted to flat group delay designs [3].

Composite right/left-handed (CRLH) transmission line

(TL) metamaterial structures have been recently demonstrated to enable novel phase-engineered devices. Whereas resonant-type metamaterials, such as split-ring-resonator and thin-wire structures cannot support impulse operation due to their narrow bandwidth, CRLH TL metamaterials, which have already been extensively used in narrow-band applications, have a potential for unique *impulse* devices and systems, due to their very broadband characteristics.

This paper proposes the principles of CRLH TL metamaterial dispersion engineering and presents several corresponding guided-wave and radiated-wave applications.

## 2. Dispersion Engineering

### 2.1 Concept

In any dispersive medium, the group velocity  $v_g$  is a function of frequency, which results in a frequency-dependent group delay. A wide-band signal subsequently suffers from distortion in such a medium because its different spectral components travel with different group velocities. This is generally perceived as an undesirable effect and is avoided. However, if dispersion (phase) is designed in a well-controlled manner, useful components can be designed. Fig. 1 illustrates the concept of dispersion engineering, where phase manipulation provides various interesting effects and functionalities [4].

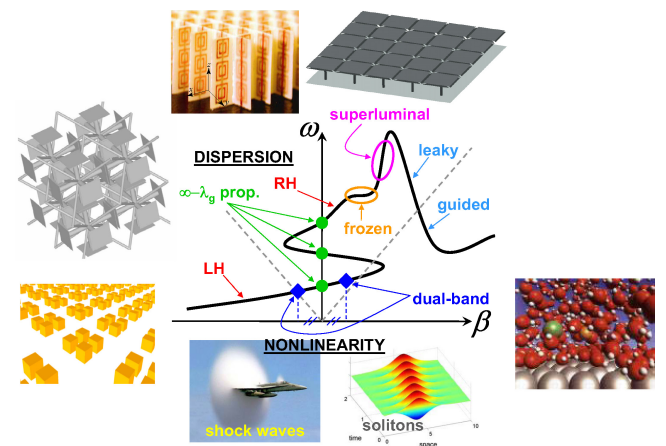


**Fig. 1.** Illustration of the dispersion engineering concept.

The dispersion relation  $\beta(\omega)$  of a medium can be expanded in Taylor series about a center (or carrier) frequency  $\omega_c$  as follows:

$$\beta(\omega) = \beta_0 + \beta_1(\omega - \omega_c) + \frac{1}{2}(\omega - \omega_c)^2 + \dots \quad (1)$$

$$\text{where } \beta_n(\omega) = \left. \frac{d^n \beta(\omega)}{d\omega^n} \right|_{\omega=\omega_c}.$$

The Taylor series coefficients  $\beta_0$ ,  $\beta_1$  and  $\beta_2$  represent the phase velocity parameter, the group velocity parameter, and the group velocity dispersion, respectively.  $\beta_1^{-1}$  is the propagation velocity, while  $\beta_2$  is a measure of the dispersion strength. Based on this Taylor expansion, various systems can be designed by using different Taylor coefficients, as shown in Tab. 1.

## 2.2 Microwave Dispersive Devices

In microwave applications, dispersion can be achieved using the different technologies such as surface acoustic wave (SAW) devices, magneto-static wave (MSW) devices and reflection-type devices such as chirped microstrip line and coupler structures. Each of these technologies has advantages and disadvantages.

SAW devices [5], thanks to their slow-wave characteristics, provide large delays ( $\approx 1\mu\text{s}$ ), and hence a large time-bandwidth product, while also having a compact size. However, they are restricted to narrow-band (2 GHz) and low-frequency applications ( $< 2$  GHz) due to limitations of current photolithography processes.

MSW devices [6] can be employed for high-frequency and wide-band operation, while also achieving high time-bandwidth product. However, in addition to being lossy, they require a permanent magnet, which is bulky and renders planar fabrication difficult.

In contrast to the transmission-type SAW and MSW structures, reflection-type structures, such as multi-section coupler based structures and chirped microstrip lines, have also been reported. Coupler-based structures are composed of a number of series-connected coupled-line couplers each operating at contiguous frequencies. Thus, high frequency ( $\approx 10$  GHz) and wide-band ( $\approx 3$  GHz) operation can be achieved. However, the bandwidth is dependent on the size of the structure, i.e. more couplers leads to larger bandwidth, which also leads to long and extremely lossy structures. In order to decrease loss, high-temperature superconductors (HTS), requiring cryogenics, must be utilized, resulting in complex and expensive devices [7].

On the other hand, the chirped microstrip line [8, 9] is a simple and planar structure, which utilizes Bragg reflections based on impedance mismatch. However, similar to the coupled-line structure, its bandwidth is also dependent on size, while also being highly lossy due its operation in the stop-band and thus requiring amplifiers.

Recently, CRLH TL metamaterial structures have been

demonstrated to offer several benefits compared to the conventional approaches for dispersion-engineered microwave devices [4].

## 2.3 Transmission Line Metamaterials

The CRLH artificial TL is composed of right-handed elements ( $L_R$ ,  $C_R$ ) and left-handed elements ( $L_L$ ,  $C_L$ ) and is characterized by the following dispersion relation [1]:

$$\beta(\omega) = \frac{1}{p} \cos^{-1} \left( 1 - \frac{\chi}{2} \right) \quad (2)$$

with  $\chi = \left( \frac{\omega}{\omega_R} \right)^2 + \left( \frac{\omega_L}{\omega} \right)^2 - \kappa \omega_L^2$

where  $\kappa = L_L C_R + L_R C_L$ ,  $\omega_R = 1/\sqrt{L_R C_R}$ ,  $\omega_L = 1/\sqrt{L_L C_L}$ , and  $p$  is the unit cell size or period, and by the Bloch impedance

$$Z_B = Z_L \sqrt{\frac{(\omega/\omega_{se})^2 - 1}{(\omega/\omega_{sh})^2 - 1} - \frac{\omega_L}{2\omega} \left[ \left( \frac{\omega}{\omega_{se}} \right)^2 - 1 \right]^2} \quad (3)$$

where  $\omega_{se} = 1/\sqrt{L_R C_L}$  and  $\omega_{sh} = 1/\sqrt{L_L C_R}$ . The corresponding dispersion relation, Bloch impedance and group delay ( $\tau_g = -\partial\phi/\partial\omega$ , where  $\phi$  is the phase shift across the structure) curves are shown in Figs. 2(a), (b), and (c), respectively. As seen in Eq. (2), the CRLH TL offers an unprecedented level of dispersion (phase) control via the CRLH parameters  $L_R$ ,  $C_R$ ,  $L_L$  and  $C_L$ . The manipulation of the CRLH dispersion relation has already led to wealth of novel narrow-band devices, such as multi-band system (dual-, tri-, and quad-band), bandwidth enhancers, to name a few. This paper concentrates on impulse-regime dispersion-engineered CRLH TL systems.

Thanks to its dispersive properties and subsequent design flexibility, the CRLH transmission line provides low-loss, compact and planar dispersion-engineered solutions, avoiding frequency limitations, complex fabrication, cryogenics, circulators or amplifiers. Moreover, the CRLH TL's

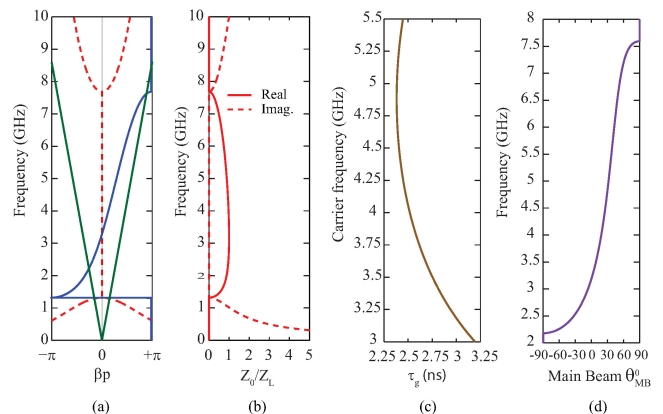


**Fig. 2.** CRLH transmission line characteristics. a) Typical dispersion curve  $\beta(\omega)$ . b) Bloch impedance  $Z_B$  normalized to  $Z_L = 50$  ohms. c) Group delay. d) Beam-scanning law.

$\beta_0$ (phase velocity parameter)	$\beta_1$ (group velocity parameter)	$\beta_2$ (group velocity dispersion)
multiband systems [1]	CW and impulse delay line (Sec. 3.1)	real-time Fourier transformer (RTFT) (Sec. 3.3)
bandwidth enhancement [1] (not discussed here)	pulse position modulator (PPM) (Sec. 3.2)	temporal Talbot effect (Sec. 3.4)
	CRLH resonator based pulse generator (Sec. 3.4)	real-time spectrum analyzers (RTSA) (Sec. 4.1)
	true time delayers (TTD) (Sec. 4.4)	frequency resolved electrical gating (FREG) (Sec. 4.2)
		spatio-temporal Talbot effect (Sec. 4.3)

**Tab. 1.** Dispersive system classification based on the Taylor coefficients of the dispersion relation – Eq. (2).

operational frequency and bandwidth dependent only on a single unit cell's right/left-handed capacitor and inductor values [1]. Thus, a compact CRLH TL can be designed to operate at high frequencies while also exhibiting wide bandwidth, as shown by the relatively constant Bloch impedance in Fig. 2(b).

A CRLH TL can also be operated in a radiative leaky-wave mode when open to free space, since the CRLH dispersion curve (Fig. 2(a)) penetrates into the fast-wave region,  $\omega \in [\omega_{BF}, \omega_{EF}]$ . The resulting leaky-wave antenna (LWA) radiates from backfire ( $\theta = -90^\circ$ ) to endfire ( $\theta = +90^\circ$ ) including broadside ( $\theta = 0^\circ$ ) as frequency is scanned from  $\omega_{BF}$  (where  $\beta = -k_0$ ) to  $\omega_{EF}$  (where  $\beta = +k_0$ ) [19, 1], following the scanning law

$$\theta(\omega) = \sin^{-1} \left[ \frac{\beta(\omega)}{k_0} \right], \quad (4)$$

which is plotted in Fig. 2(d). The CRLH LWA offers three benefits: 1) full-space radiation from backfire to endfire including broadside in the fundamental mode, offering a simple and real-time frequency-space separation mechanism; 2) frequency and bandwidth scalability, allowing to handle ultra-wideband signals; 3) simple and compact design and implementation.

According to Eq. (4), if the CRLH LWA is excited by a pulse signal, the various spectral components of the signal radiate in different directions at any particular instant. Thus, the CRLH LWA performs a *real-time spatial-to-spectral decomposition* of the signal following the beam-scanning law of the LWA as shown in Fig. 3. In this sense, the CRLH LWA operates similarly to a diffraction grating, but with a much simpler excitation mechanism.

### 3. Guided-Wave Applications

#### 3.1 Frequency Tunable Impulse Delay Line

The most important property of a dispersive structure is its frequency-dependent group delay. In the case of a balanced CRLH transmission line ( $L_R C_L = L_L C_R$ ), the group velocity of a modulated signal propagating along the structure

is obtained by taking the inverse derivative of the propagation constant with respect to frequency, as given in Eq. (2), evaluated at the carrier frequency. The corresponding group delay for the modulated signal is

$$\tau_g(\omega_c) = \frac{N}{\sin(\beta p)} \left( \frac{\omega_c}{\omega_R^2} + \frac{\omega_L^2}{\omega_c^3} \right) \quad (5)$$

where  $N$  represents the number of unit cells of the line. Thus, the time delay experienced by the modulated signal depends on the carrier frequency and may therefore be tuned by varying the carrier frequency  $\omega_c$ .

A frequency-dependent group delay tunable delay line system, introduced in [10], [11] is shown in Fig. 4(a). This system works both for continuous-wave signals and broadband impulse signals, as shown in Fig. 4(b), where the delay is tuned by the carrier frequency of the modulated signal.

This system offers several advantages over conventional systems where it is broadband with good matching, operational at high frequency, and is suitable for any planar circuit implementation technology. In addition, it offers variable tuning delay without changing the characteristics of the dispersive medium, thereby preserving good matching throughout the tuning band.

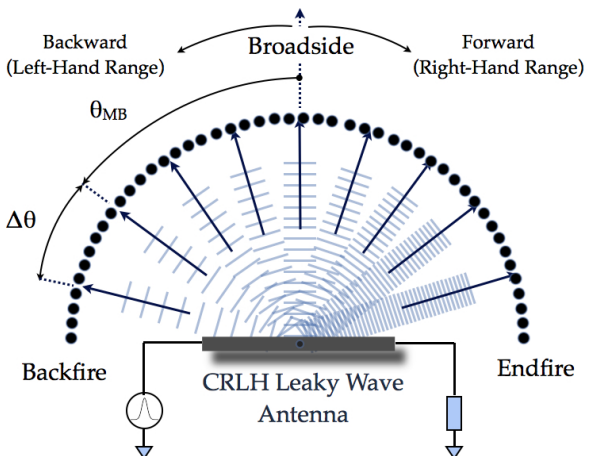


**Fig. 3.** Spectral decomposition of a pulse obtained by the frequency-space mapping property (Fig. 2.d) of a CRLH leaky-wave antenna (LWA).

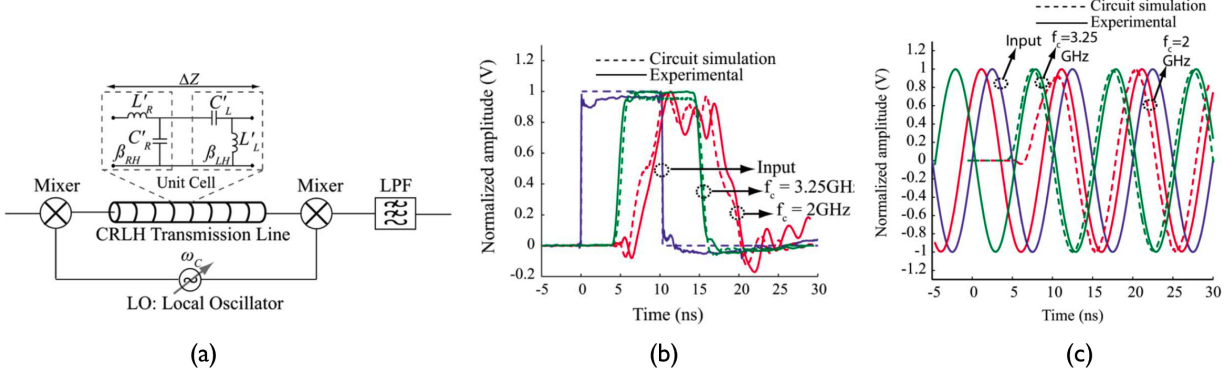


**Fig. 4.** CRLH tunable delay line system. a) Schematic. Time delayed waveforms for different carrier frequencies (experimental and circuit model) for (b) a pulse and (c) a continuous wave.

### 3.2 Pulse-Position Modulator

Extending further on the frequency dependent group delay concept in CRLH TL, a pulse-position modulator was demonstrated in [12].

Fig. 5(a) shows the block diagram of a CRLH dispersive delay line PPM transmitter. This transmitter operates as follows for an  $M$ -ary modulation scheme. A frequency source generates  $2^M$ ,  $\omega_{c,s} \in (\omega_0, \omega_1, \dots, \omega^{2M-1})$  carrier frequencies to code the  $2^M$  states. These  $2^M$  frequencies are mixed with a gaussian pulse signal  $a(t)$  from a pulse generator by a mixer. The resulting frequency-modulated gaussian pulse signal  $c(t)$  at the output of the mixer enters a dispersive CRLH transmission line. The line delays this signal  $c(t)$  unequally for the different carrier frequencies. As a result, the modulated gaussian pulse signal  $d(t)$  at the output of the line exhibits different time delays (i.e., a different pulse position in time) for different data bits. This is the basis of PPM. Finally, the time-encoded gaussian pulse signal is transmitted by a wide-band antenna. Fig. 5(b-d) demonstrate the successful encoding of a random information digital stream for the two cases of binary ( $M=2$ ) and quaternary ( $M=4$ ) PPM schemes [12].

The proposed PPM transmitter exhibits three important advantages over conventional PPM techniques. First, the CRLH dispersive delay line, being constituted of purely passive elements, does not consume any DC power and also does not generate any noise. Second, in contrast to discrete delay achieved by logic inverters or switches, this line provides a continuously tunable time delay, as shown by Fig. 2(c), where  $\tau_g$  may be continuously varied. Third, as consequence of its continuous delay, the proposed system has an inherent capability to support arbitrary  $M$ -ary PPM, where required time delays are achieved by simply mapping each data bit to a single carrier frequency within the continuous operating frequency range.

### 3.3 Frequency Discriminator and Real-Time Fourier Transformer

One of the classical applications of dispersive delay

lines is in compressive radar. Recently, a compressive radar architecture based on the CRLH dispersive delay line was proposed and experimentally demonstrated [13]. The system schematic is shown in Fig. 6(a).

The system works as follows. It employs two different delay lines with oppositely sloped group delay profiles ( $\tau_g$  vs  $\omega$  curves). The receiving frequencies  $f_1, f_2, \dots, f_n$  to be discriminated at the receiving antenna are mixed with a chirped impulse modulated at a fixed frequency  $f_0$ , which is obtained by impulsing the delay line #1 (from the chirp generating circuit). The mixed signal is then inputted to a second delay line #2 exhibiting an opposite group-delay profile compared to delay line #1. Due to this opposite group delay profile, the inputted chirped signal is compressed in time and results in distinct compressed pulses, each corresponding to the frequency  $f \in (f_1, f_2, \dots, f_n)$ . Due to this action of pulse compression, each frequency is mapped onto time according to the mapping function  $\omega = t/C$ , where  $C$  is the dispersion slope of the dispersive delay lines. Fig. 6(b) shows the output of this system for two input frequencies  $f_1$  and  $f_2$  when they are inputted separately and simultaneously. In both cases, a corresponding peak in time is observed corresponding to the input frequencies to be discriminated [13].

A frequency discriminator is a specific example of a more general class of systems called a Real-Time Fourier Transformers (RTFT) [14]. In a RTFT system, when a time limited signal is propagated through a second-order dispersive medium with sufficient dispersion  $\beta_2$ , the time signal at the output of the dispersive medium is directly proportional to the Fourier transform of the original input signal and as a result all frequencies are mapped to time. This more general RTFT principle also applies to a CRLH TL, as suggested in [15].

### 3.4 Pulse Generators

Two classes of pulse generators are described based on two different fundamental principles employing the dispersive properties of the CRLH TL. The first technique is based on the temporal Talbot effect, which uses first order disper-

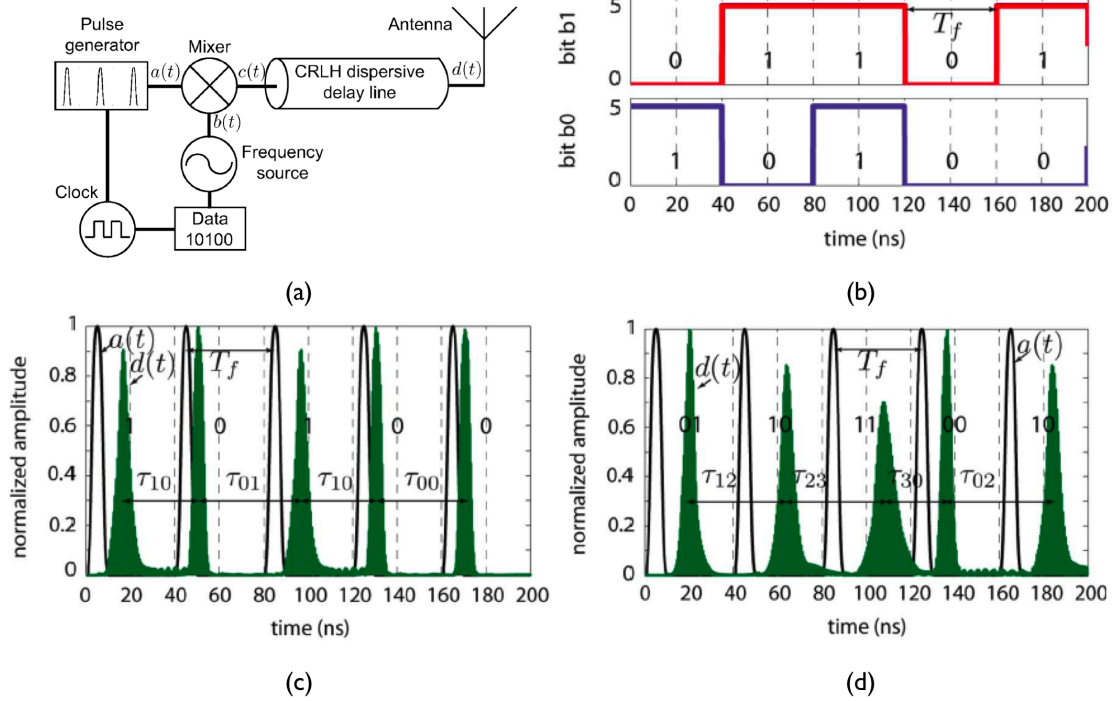


**Fig. 5.** CRLH dispersive delay line pulse position modulation (PPM) transmitter. a) System schematic. b) Information data test stream  $b_1$  and  $b_0$ . c) Circuit simulation results for binary PPM with time intervals of transition between states  $\tau_{01} = 46.41\text{ ns}$  and  $\tau_{10} = 33.59\text{ ns}$ . d) Circuit simulation results for quaternary PPM with time intervals of transition between states  $\tau_{12} = 44.19\text{ ns}$ ,  $\tau_{23} = 44.24\text{ ns}$ ,  $\tau_{30} = 27.28\text{ ns}$  and  $\tau_{02} = 44.58\text{ ns}$ .

sion (i.e. group velocity dispersion parameter  $\beta_2$ ) [16], and the second is based on the CRLH resonator inspired from optical pulsed laser systems and resonant cavities [17].

The first approach is based on well known spatial Talbot effect [18]. The temporal counterpart of this effect occurs when a periodic temporal signal propagates through a dispersive medium with second-order dispersion (i.e.  $\beta_2$ ). An input pulse train with period  $T_0$  and pulse width  $\Delta T$  is exactly replicated along the medium at periodic distances  $n z_T$  ( $n \in N$ ), where  $z_T = T_0^2 / |\beta_2|$  is called the basic Talbot distance. In addition to this integer effect, a Talbot effect with increased repetition rate of  $m$  pulses by  $T_0$  appears at the fractional distances  $z_F = (s/m)z_T$  ( $s, m \in N$ ) if  $s/m$  is an irreducible fraction and under the condition that  $m < T_0/T$ . This fractional Talbot effect may thus be used to increase the repetition rate of a periodic optical pulse train. The CRLH TL provides the required first-order dispersion (i.e. group velocity dispersion parameter  $\beta_2$ ) for Talbot self-imaging. Based on the fractional temporal Talbot effect in CRLH TL, a high speed pulse generator, proposed in [16], is shown in Fig. 7(a), where a modulated periodic pulse train is inputted to a CRLH TL. Fig. 7 (b) shows the generated pulse trains at various Talbot distances (integer and fractional) where higher repetition rate is obtained for the fractional Talbot case.

The second system is based on an impulse-regime res-

onator system as shown in Fig. 8(a). The resonator is realized by terminating the transmission line at both ends by an open circuit. Initially, a fast switch injects the input pulse into the resonator. Once the pulse has been injected into the resonator, the switch is set to a high impedance  $Z_R$ , which reflects most of the energy back into the line, and transmits only a small amount of energy, which is then amplified, into the load  $Z_L$ . The resonator acts as a cavity discretizing the input pulse spectrum leading to generation of periodic signal in time. The output repetition rate  $T_p$  is simply given by the round trip delay of the signal along the line and is thus given by  $T_p = 2\ell/v_g(\omega)$ , where  $\ell$  is the length of the transmission line and  $v_g(\omega)$  is the group velocity along the TL.

This principle in general is applicable to any kind of TL, dispersive or non-dispersive. Although the resonator principle holds in general for different transmission lines technologies, we used a CRLH TL, because it provides additional functionalities, such as pulse delay tunability, resulting in variable output repetition rates which is directly evident from its frequency dependent group velocity  $v_g(\omega)$  (or  $\tau_g(\omega)$ ) as shown in Fig. 2(c) resulting in tunable output repetition rate  $T_p(\omega)$ . This behavior can not be obtained with conventional non-dispersive transmission lines. This principle of pulse generation is demonstrated in Fig. 8(b) where a train of gaussian pulses is generated from the system schematic shown in Fig. 8(a).

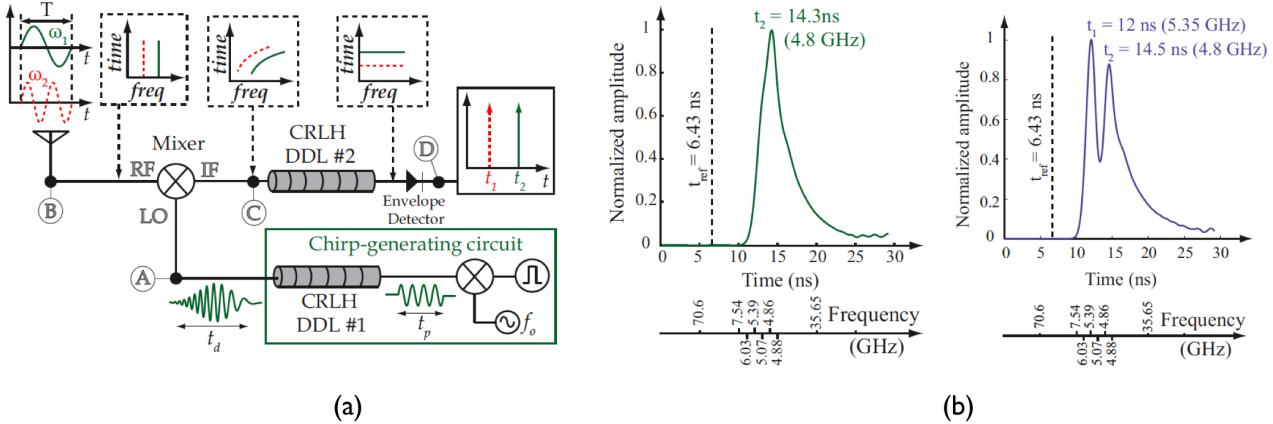


**Fig. 6.** Frequency discriminator based on the compressive receiver principle. a) System schematic. b) Circuit simulation results at the output of the envelope detector for  $f_1 = 4.8$  GHz only, and  $f_1 = 5.35$  GHz and  $f_2 = 4.8$  GHz simultaneously, respectively.

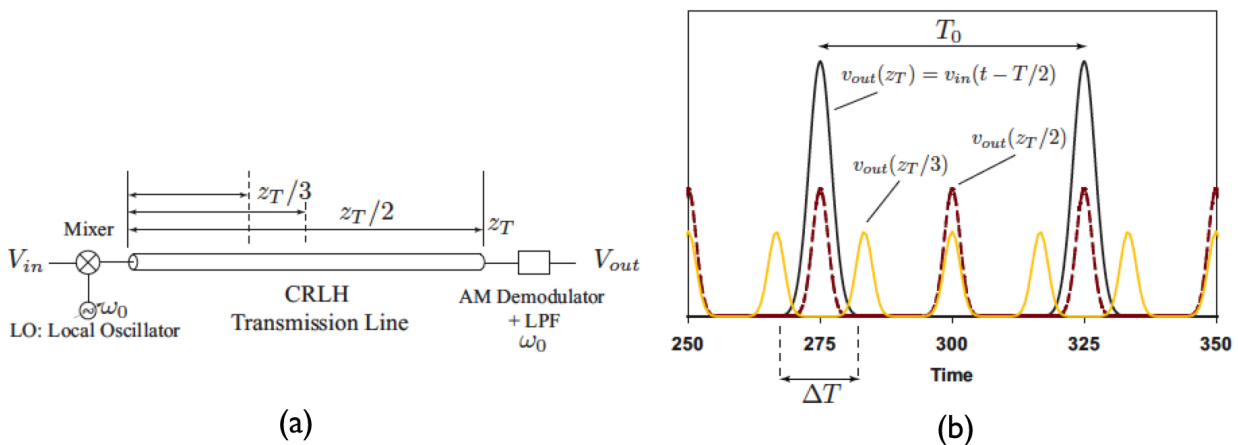


**Fig. 7.** Talbot effect in a CRLH TL system with input pulse train. a) CRLH TL with length corresponding to the basic Talbot distance  $z_T$ . b) Time-signal at various positions along the TL [integer ( $z_T$ ) and fractional ( $z_T = z_T/2, z_T/3$ ) Talbot distances].

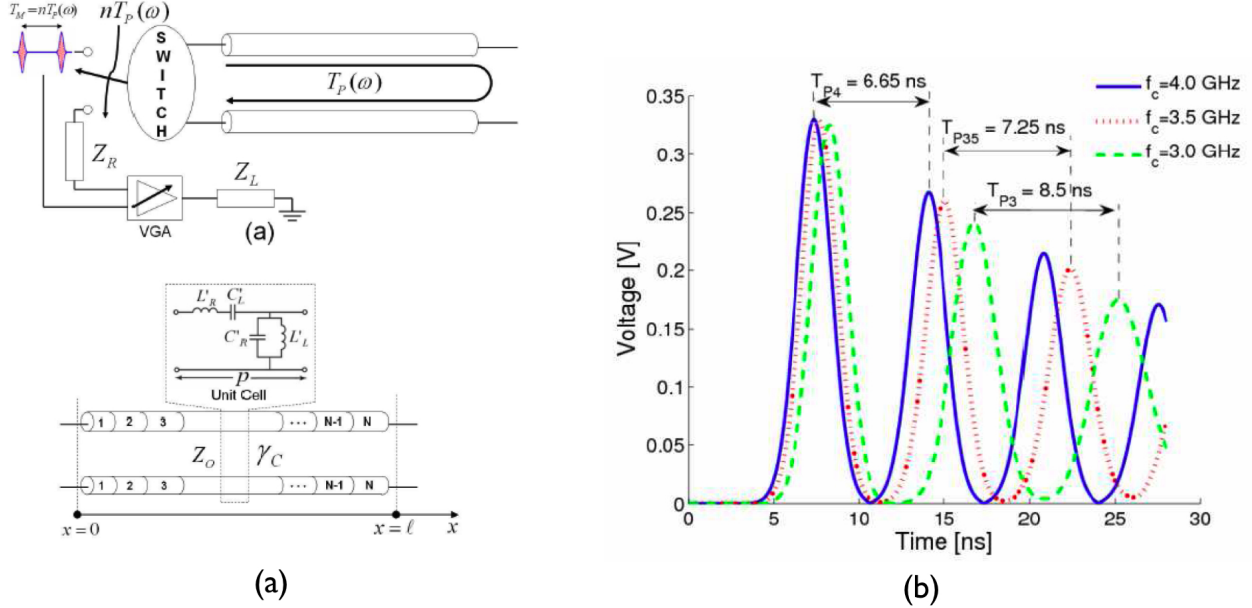


**Fig. 8.** CRLH resonator based pulse rate multiplicator. a) System schematic. b) Gaussian waveforms ( $\sigma_s = 1.0$  ns) at the output (ZR) of the CRLH resonator for different carrier frequencies showing the tunability of the system. The CRLH line is composed of 40 unit cells with circuital parameters defined in [17]. The generator impedance is  $Z_g \approx \infty$  and the load impedance is  $Z_R = 500 \Omega$ .

## 4. Radiated Wave Applications

### 4.1 Analog Real-Time Spectrum Analyzer

Most of today's ultra-wideband systems, such as compressive radars, security and instrumentation systems, and EMI/EMC, deal with non-stationary signals exhibiting rapid spectral variations in time. In order to effectively control such signals, time information and spectral information are simultaneously needed. Thus, a real-time spectral analyzer is required to detect and monitor such transient signals with rapid time variations providing the evolution of instantaneous frequencies in real time.

The *joint time-frequency representation* allows to analyze such non-stationary signals and can be obtained using *spectrogram algorithms*. Mathematically, the spectrogram of a signal  $x(t)$  is calculated using

$$S(\tau, \omega) = \left| \int_{-\infty}^{\infty} x(t)g(t-\tau)e^{-j\omega t} dt \right|^2 \quad (6)$$

where  $g(t)$  is a gate function.

The spectrograms obtained from this approach suffers from the well-known fundamental “uncertainty principle” limitation [20]. This principle implies an inherent trade-off between time resolution and frequency resolution, where increasing time resolution decreases frequency resolution, and vice-versa.

Recently, based on the spectral-spatial decomposition property of the CRLH LWA, a novel analog real-time spec-

trum analyzer (RTSA) was proposed and experimentally demonstrated [22], [21]. The proposed CRLH RTSA is shown in Fig. 9. It is based on the following three successive operations:

1. Spectral-spatial decomposition using a CRLH LWA to discriminate the frequency components of the testing signal. As the testing signal propagates along the LWA, its various spectral components are radiated in space following the beam-scanning law.
2. Probing and monitoring of the time variation of each frequency component. Probing is achieved by antenna receivers, while monitoring is performed by envelope demodulation;
3. Post-processing (power normalization taking into account the frequency dependent gain of the LWA, and spectrogram linearization to correct for the nonlinear beam-scanning law), including analog/digital conversion, data processing, and display.

To demonstrate the RTSA principle shown in Fig. 9, the CST Microwave Studio full-wave simulator (finite integration time domain) is used and various time-domain waveforms are injected into the LWA as testing signals. The obtained spectrograms are shown in Fig. 10 for several time domain signals where a faithful representation of rapid complex spectral variations can readily be seen.

The proposed analog RTSA system offers several advantages compared to the conventional real-time analysis systems such as digital RTSAs. Firstly, it is a completely *analog* system and does not require any digital computa-

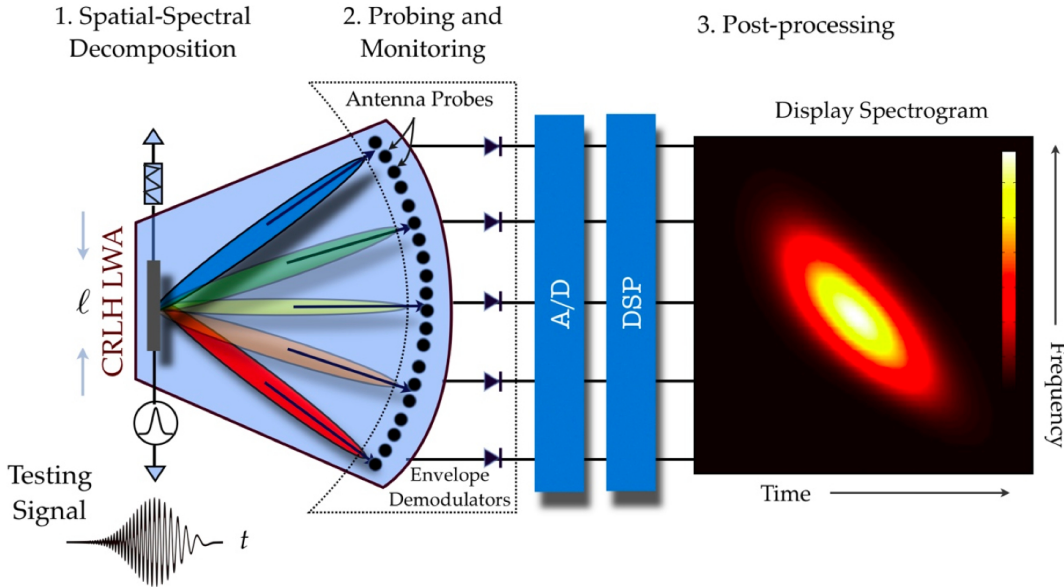


**Fig. 9.** Analog RTSA showing the CRLH LWA, the antenna probes, the envelope detectors, the A/D converters, the DSP block, and the display with the spectrogram.

tion thus requiring neither fast processors nor large memory. Moreover, since the measurements are single-shot (no memory buffers), the systems operate in a real-time mode. Secondly, the proposed RTSA is a frequency-*scalable* system. The CRLH LWA may be designed at any arbitrary frequency to meet the requirements of the specific applications [1]. Thirdly, the proposed RTSA is inherently *broadband or ultra-wideband*, with bandwidth controllable by proper design of the CRLH transmission line.

The time and frequency resolution of spectrograms generated using this technique unfortunately depends on the physical length of the CRLH LWA. This dependence of the spectrogram on the length is suppressed in the system described next.

## 4.2 Frequency-Resolved Electrical Gating

Frequency resolved electrical gating (FREG) is the microwave counterpart of the optical frequency resolved optical gating (FROG) system used for the characterization of ultrashort optical pulses [23]. This system also computes the spectrogram of a broadband signal. In order to compute a spectrogram of a signal  $A(t)$ , a gating function  $g(t)$  is always required, as shown in Eq. (6). Whereas RTSA is based on a space-gating principle, FREG is self-gating system: instead of using a separate time signal for the gate function, it used the *envelope of the testing signal* itself as the gating function, i.e.  $g(t) = |A(t)|$ . The spectrogram of a signal  $A(t)$  is thus modified as

$$S(\tau, \omega) = \left| \int_{-\infty}^{\infty} A(t) |A(t - \tau)| e^{-j\omega t} dt \right|^2. \quad (7)$$

A CRLH LWA FREG system, also using the spatial-spectral decomposition property of the CRLH LWA, was recently

proposed [24]. This system is depicted in Fig. 11. The testing signal, whose spectrogram is to be generated, is split into two channels. One of the channels is envelope-detected and passed through a tunable delay line. The two channels are then mixed together. The mixer thus performs the self-gating process at a given time delay instant  $\tau$ . The self-gated signal is then injected into a CRLH LWA which spectrally resolves it in space. Once the frequency components are separated in space, antennas circularly placed in the far-field of the LWA receive the different frequency components corresponding their angular position. All the received signals are then digitized and summed, before being stored for spectrogram display.

The FREG system exhibits significant advantages over the analog RTSA system and purely digital systems. Due to the self-gating process, neither the time and nor the frequency resolutions of the generated spectrogram depend on the physical length of the antenna. The time and frequency resolutions are thus dependent only on the time signal itself and the hardware dependence spectrogram is suppressed. The LWA simply plays a role of spectral decomposer which, when longer (higher directivity), provides better separation of frequencies in space. However, since it uses a multi-shot measurement procedure, where the testing signal is gated several times with different time delays  $\tau$ , the FREG system requires a periodic signal. This is the main constraint of the FREG. Fig. 12 shows FREG-generated spectrograms demonstrating the capability of the proposed FREG system to analyze a wide variety of non-stationary signals [24].

## 4.3 Spatio-Temporal Talbot Effect

The spatial-temporal Talbot phenomenon occurs when the CRLH LWA array elements, acting as the microwave counterpart of optical diffraction gratings, are simultane-

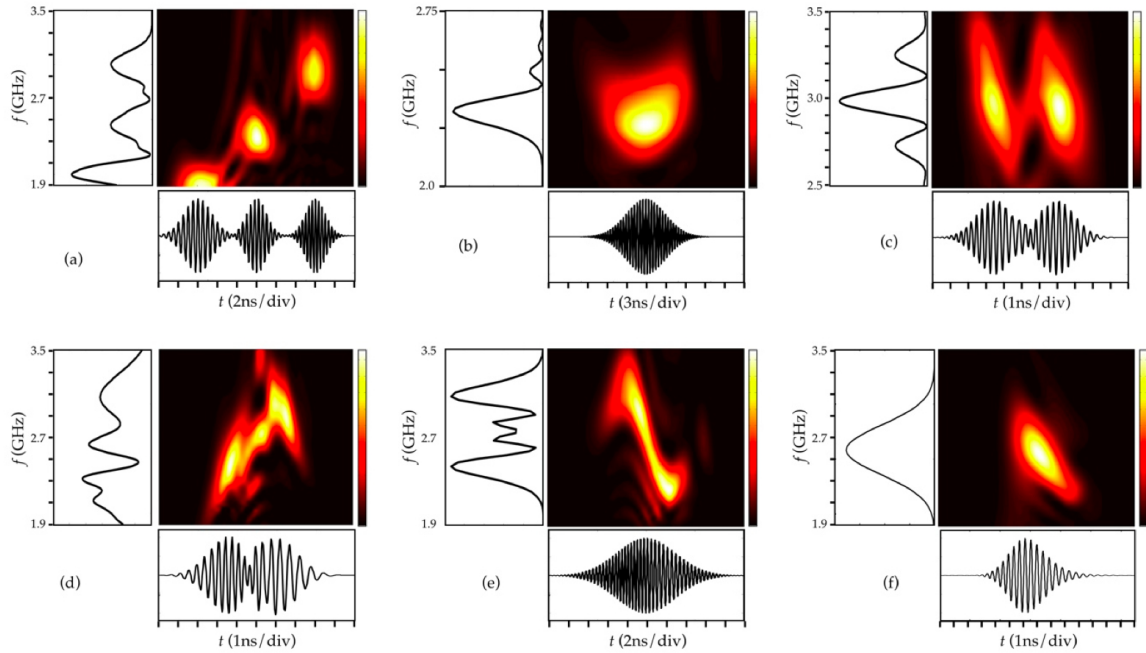


**Fig. 10.** Full-wave (CST Microwave Studio) spectrograms. a) Multiple modulated gaussian pulses. b) Nonlinear cubically chirped gaussian pulse. c) Doubly negative chirped gaussian pulses. d) Oppositely chirped gaussian pulses. e) Self-phase modulated pulses. f) Dispersed pulse through a CRLH TL. The input signals are generated by the time domain functions and parameters provided in [22].

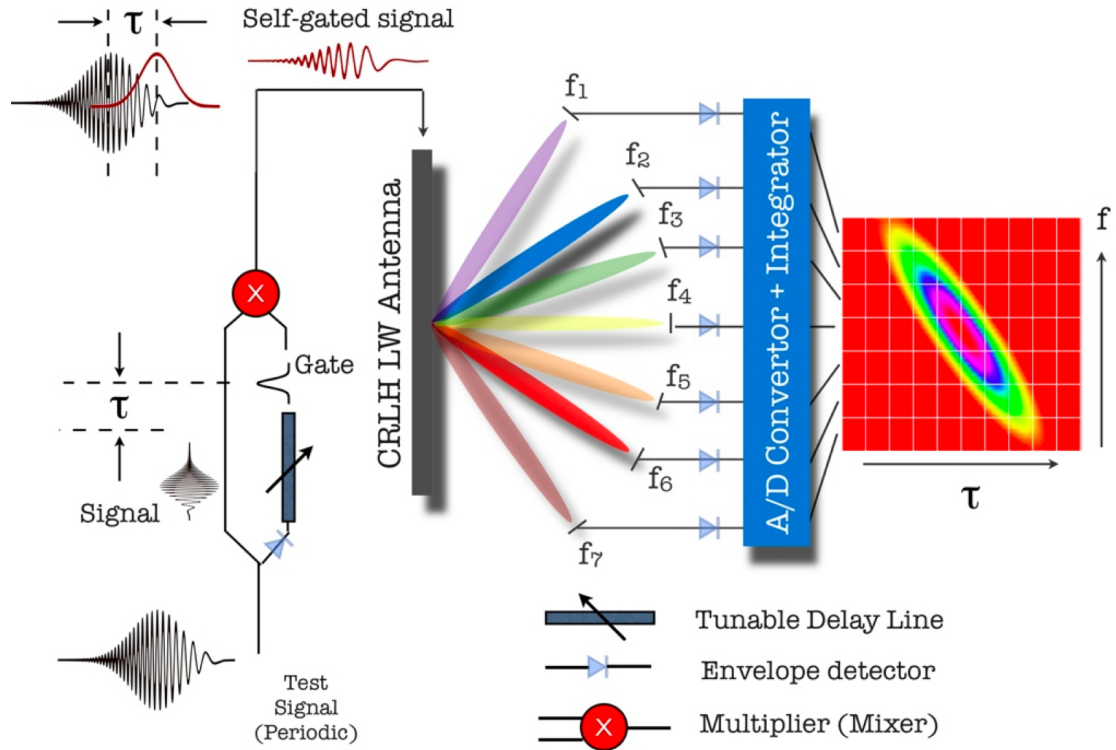


**Fig. 11.** Frequency resolved electrical gating (FREG) system.

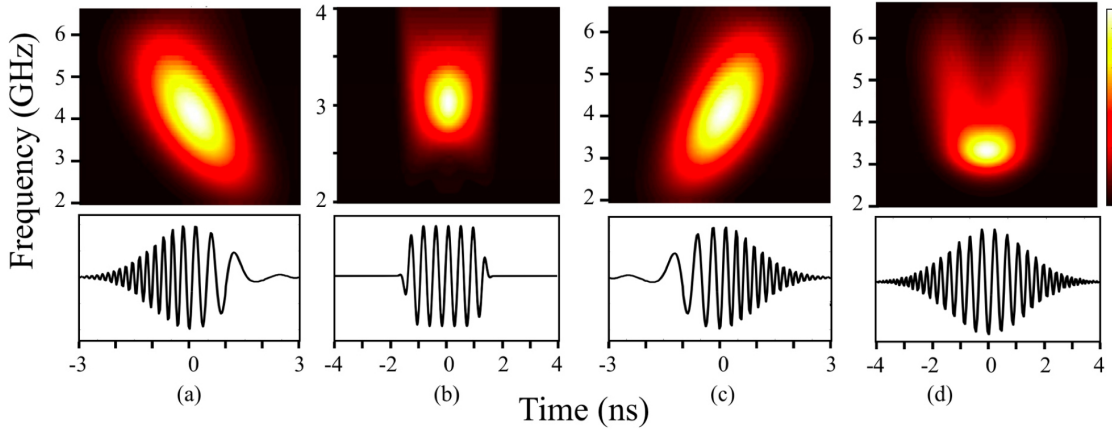


**Fig. 12.** Simulated spectrograms from a FREG system for a) a down-chirped gaussian pulse ( $C_1 = -10$ ,  $C_2 = 0$ ,  $f_0 = 4$  GHz), b) a non-chirped super-gaussian pulse ( $C_1 = C_2 = 0$ ,  $f_0 = 3$  GHz), c) an up-chirped gaussian pulse ( $C_1 = +10$ ,  $C_2 = 0$ ,  $f_0 = 4$  GHz), d) a cubically chirped gaussian pulse ( $C_1 = 0$ ,  $C_2 = 0.25 \times 10^{28}$ ). All the pulses have a full width half maximum duration of 1 ns with a initial pulse offset of  $t_0 = 6.5$  ns.

ously fed with a single temporal pulse. Due to the spatial-spectral decomposition property of the antennas, the pulses are spectrally decomposed in space following the CRLH beam-scanning law of Eq. (4), as illustrated in Fig. 13. The spatial beams corresponding to the different temporal frequencies interfere in space creating an interference pattern, i.e. produce the spatial Talbot effect. Due to the non-zero bandwidth of the input pulse, the Talbot planes occurring in the case of the monochromatic wave are replaced by Talbot zones corresponding to the bandwidth of the temporal pulse. This Talbot effect is mixed spatial-temporal since the Talbot zones are localized both in space and time. [25]. These Talbot planes are located at propagation distances given by:

$$z_T = \frac{s}{m} \frac{\Delta x^2}{\lambda_0} \quad (8)$$

where  $\Delta x$  is the separation between the neighboring antennas in the LWA array and  $\lambda_0$  is the modulation frequency of the input temporal pulse which should also be the transition frequency of the CRLH LWA.

Figs. 13 (b-d) show the simulated radiation fields for different Talbot planes using an efficient time-domain Green's function approach [26]. The original field distribution is either self-imaged at the basic Talbot plane ( $z = z_T$ ) or is imaged with higher periodicity in space  $z = z_T/m$ ,  $m$  being an integer.

#### 4.4 Analog True-Time Delayer

The array factor of a linear phased-array antenna of  $K$  elements is given by

$$AF(\theta) = \sum_{n=1}^N e^{j(n-1)\phi}, \text{ with } \phi = k_0 d \cos \theta + \phi \quad (9)$$

where  $k_0$  is the free-space number,  $\phi$  is the element to element phase shift,  $d$  is the element separation and  $\theta$  is the angle of radiation from endfire. The main beam direction cor-

responding to maximum gain occurs at  $\theta = \theta_0$  when  $\phi = 0$  leading to

$$\theta_0 = \cos^{-1} \left( \frac{\phi c}{2\pi f_{RF} d} \right) \quad (10)$$

where  $f_{RF}$  is the radiation frequency and  $c$  is the velocity of light in free space. If  $\phi$  remains constant, as in conventional phase shifters, a variation in  $f_{RF}$  induces an inverse variation in  $\theta_0$  and hence the beam squints, i.e. its different spectral components radiate in slightly different directions. In contrast, if true-time delayers with delay  $\tau_g$  and corresponding phase shift  $\phi = 2\pi f_{RF} \Delta \tau_g$  are used instead of phase shifters, Eq. (10) leads to the following expression for  $\theta_0$ :

$$\theta_0 = \cos^{-1} \left( \frac{\Delta \tau_g c}{d} \right), \quad \text{with } \Delta \tau_g \neq \Delta \tau_g(f) \quad (11)$$

where  $\Delta \tau_g = \tau_{g,n+1} - \tau_{g,n}$  is the phased array's element-to-element time delay difference. Therefore by controlling  $\Delta \tau_g$  (by controlling  $f_{LO,K}$ ), the main beam scans in a desirable direction  $\theta_0$  and the main beam direction  $\theta_0$  has been rendered independent of  $f_{RF}$ , hence eliminating beam-squinting.

This principle was recently applied in [27], where the CRLH based tunable delay line configuration described in Sec. 3.1 and shown in Fig. 14 [11] was employed as the phase shifting device. Figs. 14(a) and (b) show the CRLH true-time delay system and its proposed implementation in a phased array, respectively. By operating the CRLH transmission line in the frequency bandwidth exhibiting an approximately linear group delay (or quadratic phase), the beam squinting can be suppressed, as shown in Eq. (11).

Fig. 14(c) illustrates beam-squinting in a phased array employing ideal phase shifters where  $\Delta \phi$  is constant with frequency. With  $f_{RF} = 5$  GHz and  $\delta f_{RF} = \pm 0.5$  GHz, the beam squints by a total of  $15^\circ$ . By employing the proposed CRLH TD system, Fig. 14(d) illustrates the suppression of beam-squinting.

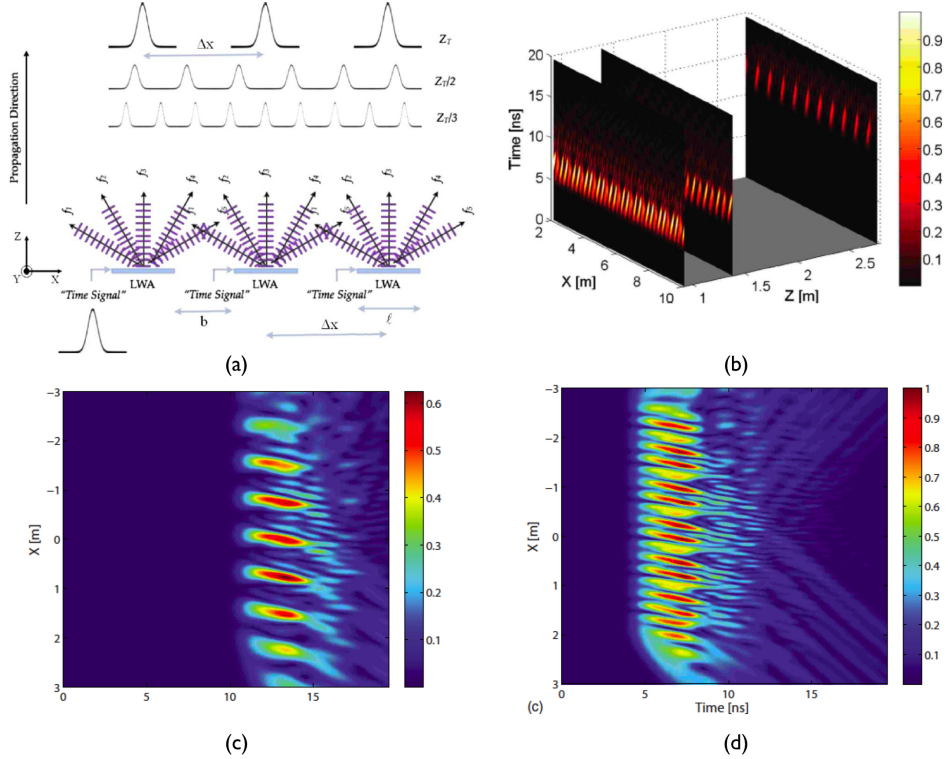


**Fig. 13.** Spatio-temporal Talbot effect. a) System schematic showing an array of LWAs placed at  $z = 0$  along the  $x$ -axis, radiating in space for an impulse input. b) Field magnitude radiated by the CRLH LWA array for an antenna element spacing of  $b = 0.5$  m and modulated gaussian pulse excitation as a function of the position  $x$  and the time at the propagation distance  $z = z_T = 2.738$  m,  $z = z_T/2 = 1.369$  m and  $z = z_T/3 = 0.9127$  m. c) Field magnitude in the integer talbot plane  $z = z_T$  and d) fractional Talbot place  $z = z_T/3$ .

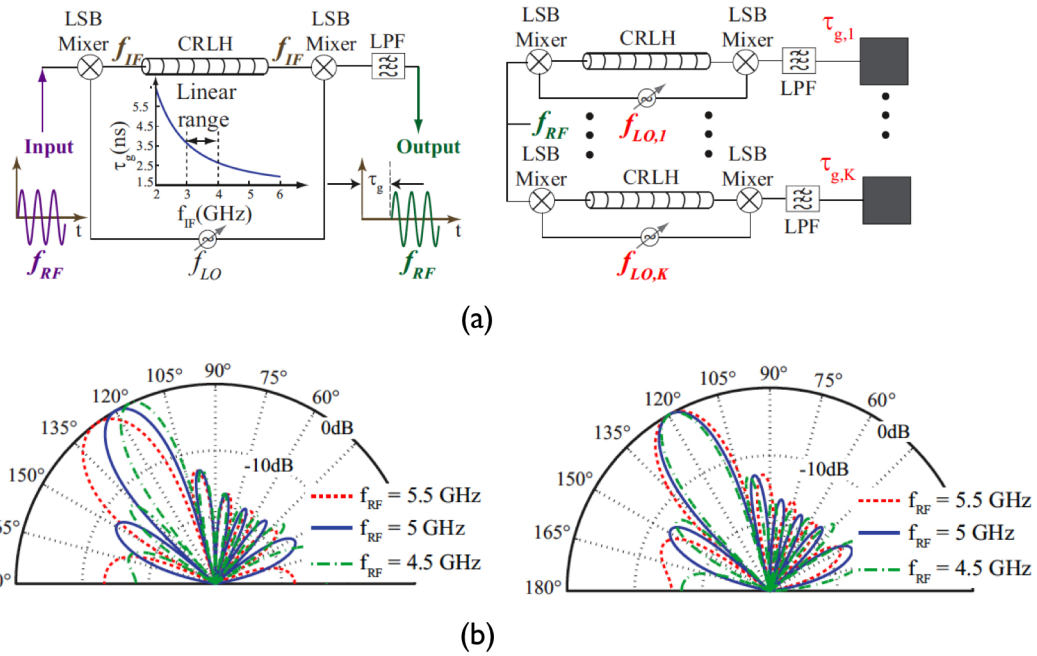


**Fig. 14.** Tunable CRLH TD system (a) Single TD system with corresponding  $\tau_g$  (IF). (b) K-element TD systems for phased array scanning. Computed beam-squinting radiation patterns with  $K = 8$  and  $f_{RF} = \pm 0.5$  GHz for ideal phase shifters ( $\phi \neq \phi(f_{RF})$ ) and the CRLH TD system.

## 5. Conclusions

Several novel dispersion-engineered CRLH TL metamaterial analog signal processing systems, exploiting the broadband dispersive characteristics and design flexibility of CRLH TLs, have been presented. They represent a new class of impulse-regime metamaterial structures, while previously reported metamaterials were mostly restricted to the harmonic regime.

## References

- [1] CALOZ, C., ITOH, T. *Electromagnetic Metamaterials, Transmission Line Theory and Microwave Applications*. Wiley and IEEE Press, 2006.
- [2] AGARWAL, G. P. *Nonlinear Fiber Optics*. Academic Press, 2005.
- [3] MATTHAIE, G. L., YOUNG, L., JONES, E. M. T. *Microwave Filters, Impedance-Matching Networks, and Coupling Structures*. Dedham: Artech House, 1964.
- [4] GUPTA, S., CALOZ, C. Dispersion and nonlinearity engineered metamaterial devices. In *Proc. Metamaterials 2007*, Rome (Italy), 2005, p. 627 - 630.
- [5] DOLAT, V. S., WILLIAMSON, R. C. A continuously variable delay-line system. In *Proc. of the IEEE Ultrasonics Symp.*, Annapolis, 1976, p. 419 - 423.
- [6] ISHAK, W. S. Magnetostatic wave technology: A review. *Proc. of the IEEE*, 1998, vol. 76, no. 2, p. 171 - 187.
- [7] WITHERS, R. S., ANDERSON, A. C., GREEN, J. B., REIBLE S. A. Superconductive delay-line technology and applications. *IEEE Trans. on Magnetics*, 1985, vol. MAG-21, no. 2, p. 186 - 192.
- [8] LASO, M. A. G., LOPETEGI, T., ERRO, M. J., BENITO, D., GARDE, M. J., MURIEL, M. A., SORILLA, M., GUGLIELMI, M. Real-time spectrum analysis in microstrip technology. *IEEE Trans. Microw. Theory and Techniques*, 2003, vol. 51, no. 3, 2003, p. 705 - 717.
- [9] COULOMBE, M., CALOZ, C. Reflection-type artificial dielectric substrate microstrip dispersive delay line (DDL) for analog signal processing. To appear in *IEEE Trans. Microw. Theory and Techniques*.
- [10] GUPTA, S., ABIELMONA, S., CALOZ, C. CRLH carrier-frequency tunable impulse and continuous wave delay lines. In *Proc. IEEE APS International Symposium*. Honolulu, 2007, p. 5523 - 5526.
- [11] ABIELMONA, S., GUPTA, S., CALOZ, C. Experimental demonstration and characterization of a tunable CRLH delay line system for impulse/continuous wave. *IEEE Microwave Wireless Compon. Lett.*, 2007, vol. 17, no. 12, p. 864 - 866.
- [12] NGUYEN, H. V., CALOZ, C. CRLH delay line pulse position modulation transmitter. *IEEE Microwave Wireless Compon. Lett.*, 2008, vol. 18, no. 5, p. 527 - 529.
- [13] ABIELMONA, S., GUPTA, S., CALOZ, C. Compressive receiver using a CRLH-based dispersive delay line for analog signal processing. Submitted to *IEEE Transactions on Microwave Theory and Techniques*.
- [14] JANSON, T. Real-time Fourier transformation in dispersive optical fibers. *Opt. Lett.*, 1983, vol. 8, p. 232 - 234.
- [15] ABIELMONA, S., CALOZ, C. Compressive receiver for frequency discrimination based on dispersion-engineered metamaterial delay line. In *Proc. CNC/USNC URSI National Radio Science Meeting*. Ottawa, CD-ROM.
- [16] GUPTA, S., CALOZ, C., Temporal Talbot effect in left-handed metamaterial transmission lines, in *Proc. International Symposium on Electromagnetic Theory (EMTS)*. Ottawa, 2007, CD-ROM.
- [17] GÓMEZ-DÍAZ, J. S., GUPTA, S., ALVAREZ-MELCON, A., CALOZ, C. Impulse-regime CRLH resonator and its application to a tunable pulse rate multiplicator. To appear in *Radio Science*.
- [18] TALBOT, H. F. Facts relating to optical science no. IV. *Philos. Mag.*, 1836, vol. 9, p. 401-407.
- [19] LIU, L., CALOZ, C., ITOH, T. Dominant mode (DM) leaky-wave antenna with backfire-to-endfire scanning capability. *Electron. Lett.*, 2002, vol. 38, no. 23, p. 1414 - 1416.
- [20] COHEN, L. Time-frequency distributions-a review. *Electronic Letters, Proceeding of IEEE*, vol. 77, no. 7, p. 941 - 981.
- [21] GUPTA, S., ABIELMONA, S., CALOZ, C. Leaky-wave based spectrum analyzer with unrestricted time-frequency resolution. In *Proc. IEEE MTT-S Int. Microwave Symp. Dig.* Atlanta, 2008, p. 807 - 810.
- [22] GUPTA, S., ABIELMONA, S., CALOZ, C. Microwave analog real-time spectrum analyzer (RTSA) based on the spectral-spatial decomposition property of leaky-wave structures. Submitted to *IEEE Trans. Microwave Theory Tech.*
- [23] TREBINO, R. *Frequency-Resolved Optical Gating: The Measurement of Ultrashort Laser Pulses*. Springer, 2002.
- [24] GUPTA, S., GÓMEZ-DÍAZ, J. S., CALOZ, C. Frequency resolved electrical gating (FREG) system based on a CRLH leaky-wave antenna for UWB signal characterization. To appear in *Proc. 39th European Microwave Conf. (EuMC)*. Rome, 2009.
- [25] GÓMEZ-DÍAZ, J. S., ALVAREZ-MELCON, A., GUPTA, S., CALOZ, C. Novel spatio-temporal Talbot phenomenon using metamaterial composite right/left-handed leaky-wave antennas. *J. App. Phys.*, 2008, vol. 104, p. 104901 - 104907.
- [26] GÓMEZ-DÍAZ, J. S., GUPTA, S., ALVAREZ-MELCON, A., CALOZ, C. Investigation on the phenomenology of impulse-regime metamaterial transmission lines. To appear in *Communications in IEEE Transactions on Antennas and Propagation*.
- [27] NGUYEN, H. V., ABIELMONA, S., CALOZ, C., Analog dispersive time delay for beam-scanning phased array without beam-squinting. In *Proc. Antennas Propaga. Symp.* San Diego, 2008.

## About Authors...

**Shulabh GUPTA** was born on 14th december, 1982 in India. He completed his Bachelors in Technology (B.Tech) in electronics from Indian School of Mines, India and Masters of Science (MS) in telecommunications from INRS-EMT, Université du Québec in 2004 and 2006 respectively. He is presently pursuing his Doctoral degree under the supervision of Prof. Christophe Caloz in École Polytechnique of Montréal in Canada. He has filed two patents and is a recipient of Young Scientist Award in URSI-GA, Chicago '08 and EMTS Ottawa '07. He was selected among the top-3 finalists in the "Most Creative and Original Measurements Setup or Procedure" contest at 2008 International Microwave Symposium (IMS), Atlanta, IL in 2008. His current research interest is in dispersion engineered metamaterials for ultra-wideband systems and devices and Fourier optics inspired leaky-wave structures and systems.

**Christophe CALOZ** received the Diplôme d'Ingénieur en Électricité and the Ph.D. degree from École Polytechnique Fédérale de Lausanne (EPFL), Switzerland, in 1995 and

2000, respectively. From 2001 to 2004, he was a postdoctoral research engineer at the Microwave Electronics Laboratory of University of California at Los Angeles (UCLA). In June 2004, Dr. Caloz joined École Polytechnique of Montréal, where he is now an associate professor, a member of the Microwave Research Center Poly-Grames, and the holder of a Canada Research Chair (CRC). He has authored and co-authored 350 technical conference, letter and journal papers, 7 book and book chapters, and he holds several patents. He is a Senior Member of the IEEE, a Member of the Microwave Theory and Techniques Society (MTT-S) Technical Coordinating Committee (TCC) MTT-15, a Speaker of the MTT-15 Speaker Bureau, and the Chair of

the Commission D (Electronics and Photonics) of the Canadian Union de Radio Science Internationale (URSI). He is a member of the editorial board of the International Journal of Numerical Modelling (IJNM), of the International Journal of RF and Microwave Computer-Aided Engineering (RFMiCAE), of the International Journal of Antennas and Propagation (IJAP), and of the journal "Metamaterials" of the Metamorphose Network of Excellence. He received the UCLA Chancellor's Award for Post-doctoral Research in 2004 and the MTT-S Outstanding Young Engineer Award in 2007. His research interests include all fields of theoretical, computational and technological electromagnetics engineering, with strong emphasis on emergent and multidisciplinary topics.